
Recent Results and Status of TEXONO Experiments

Venktesh Singh* and Henry T. Wong

(on behalf of the TEXONO Collaboration)

Institute of Physics, Academia Sinica, Taipei 11529, Taiwan

E-mail: vsingh@phys.sinica.edu.tw, htwong@phys.sinica.edu.tw

ABSTRACT: This article reviews the research program and efforts for the TEXONO Collaboration on neutrino and astro-particle physics. The “flagship” program is on reactor-based neutrino physics at the Kuo-Sheng (KS) Power Plant in Taiwan. A limit on the neutrino magnetic moment of $\mu_{\bar{\nu}_e} < 1.3 \times 10^{-10} \mu_B$ at 90% confidence level was derived from measurements with a high purity germanium detector. Other physics topics at KS, as well as the various R&D program, are discussed.

1. Introduction and History

The TEXONO¹ Collaboration[1] has been built up since 1997 to initiate and pursue an experimental program in Neutrino and Astroparticle Physics[2]. The Collaboration comprises more than 40 research scientists from major institutes/universities in Taiwan (Academia Sinica[†], Chung-Kuo Institute of Technology, Institute of Nuclear Energy Research, National Taiwan University, National Tsing Hua University, and Kuo-Sheng Nuclear Power Station), China (Institute of High Energy Physics[†], Institute of Atomic Energy[†], Institute of Radiation Protection, Nanjing University, Tsing Hua University) and the United States (University of Maryland), with AS, IHEP and IAE (with [†]) being the leading groups. It is the first research collaboration of this size and magnitude among scientists from Taiwan and China[3].

Results from recent neutrino experiments strongly favor neutrino oscillations which imply neutrino masses and mixings [4]. Their physical origin and experimental consequences are not fully understood. There are strong motivations for further experimental efforts to shed light on these fundamental questions by probing standard and anomalous neutrino properties and interactions. The results can constrain theoretical models which will be necessary to interpret the future precision data. In addition, these studies would also explore new detection channels to open up new avenues of investigations.

*Speaker.

¹Taiwan EXperiment On Neutrino

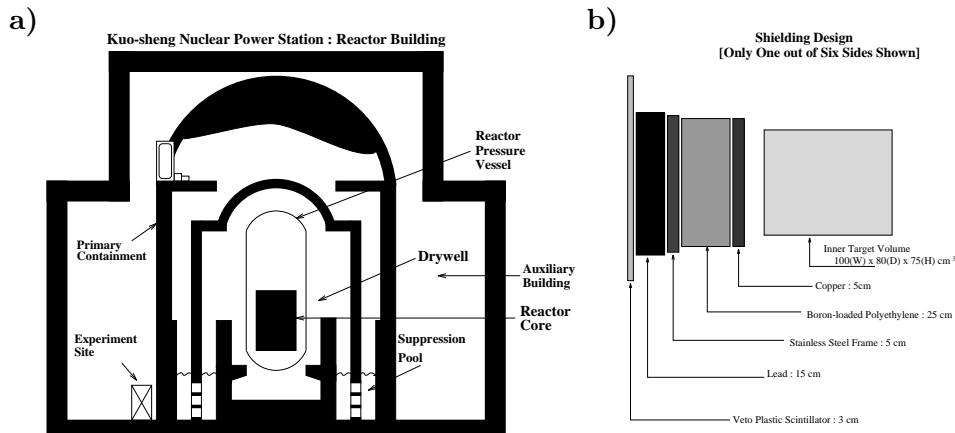


Figure 1: (a) Schematic side view, not drawn to scale, of the Kuo-Sheng Nuclear Power Station Reactor Building, indicating the experimental site. The reactor core-detector distance is about 28 m. (b) Schematic layout of the inner target space, passive shieldings and cosmic-ray veto panels. The coverage is 4π but only one face is shown.

The TEXONO research program is based on the the unexplored and unexploited theme of adopting detectors with high- Z nuclei, such as solid state device and scintillating crystals, for low-energy low-background experiments in Neutrino and Astroparticle Physics[5]. The main effort is a reactor neutrino experiment at the Kuo-Sheng (KS) Nuclear Power Station in Taiwan to study low energy neutrino properties and interactions[6]. The Kuo-Sheng experiment is the first particle physics experiment in Taiwan. In parallel to the reactor experiment, various R&D efforts coherent with the theme are initiated and pursued.

Subsequent sections highlight the results and status of the program.

2. Kuo-Sheng Neutrino Laboratory

The “Kuo-Sheng Neutrino Laboratory” is located at a distance of 28 m from the core #1 of the Kuo-Sheng Nuclear Power Station at the northern shore of Taiwan[6]. A schematic view is depicted in Figure 1a.

A multi-purpose “inner target” detector space of $100\text{ cm} \times 80\text{ cm} \times 75\text{ cm}$ is enclosed by 4π passive shielding materials which have a total weight of 50 tons. The shielding provides attenuation to the ambient neutron and gamma background, and consists of, from inside out, 5 cm of OFHC copper, 25 cm of boron-loaded polyethylene, 5 cm of steel, 15 cm of lead, and cosmic-ray veto scintillator panels. The schematic layout of one side is shown in Figure 1b.

Different detectors can be placed in the inner space for the different scientific goals. The detectors are read out by a versatile electronics and data acquisition systems[7] based on a 16-channel, 20 MHz, 8-bit Flash Analog-to-Digital-Convertor (FADC) module. The readout allows full recording of all the relevant pulse shape and timing information for as long as several ms after the initial trigger. Software procedures have been devised to extend the effective dynamic range from the nominal 8-bit measurement range provided by the FADC[8]. The reactor laboratory is connected via telephone line to the home-base

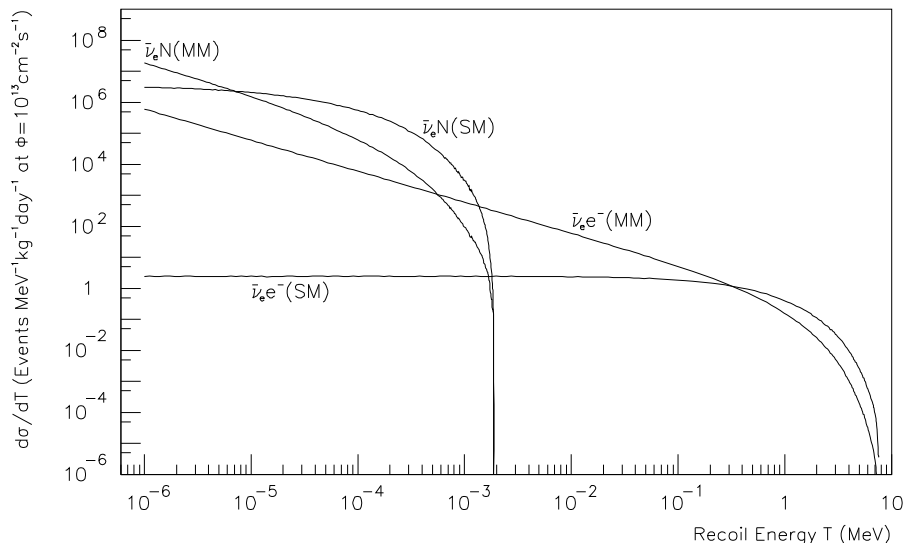


Figure 2: Differential cross section showing the recoil energy spectrum in $\bar{\nu}_e$ -e and coherent $\bar{\nu}_e$ -N scatterings, at a reactor neutrino flux of $10^{13} \text{ cm}^{-2}\text{s}^{-1}$, for the Standard Model (SM) processes and due to a neutrino magnetic moment (MM) of $10^{-10} \mu_B$.

laboratory at AS, where remote access and monitoring are performed regularly. Data are stored and accessed via the PC IDE-bus from a cluster of multi-disks arrays each with 800 Gbyte of memory.

The measure-able nuclear and electron recoil spectra due to reactor $\bar{\nu}_e$ are depicted in Figure 2, showing the effects due to Standard Model [$\sigma(\text{SM})$] and magnetic moment [$\sigma(\mu_\nu)$] $\bar{\nu}_e$ -electron scatterings[9], as well as the Standard Model neutrino coherent scatterings on the nuclei [$\sigma(\text{coh})$]. It was recognized recently[10] that due to the uncertainties in the modeling of the low energy part of the reactor neutrino spectra, experiments to measure $\sigma(\text{SM})$ with reactor neutrinos should focus on higher electron recoil energies ($T > 1.5 \text{ MeV}$), while μ_ν searches should base on measurements with $T < 100 \text{ keV}$. Observation of $\sigma(\text{coh})$ would require detectors with sub-keV sensitivities.

Accordingly, data taking were optimized for with these strategies. An ultra low-background high purity germanium (ULB-HPGe) detector was used for Period I (June 2001 till May 2002) data taking, while 186 kg of CsI(Tl) crystal scintillators were added in for Period II (starting January 2003). Both detector systems operate in parallel with the same data acquisition system but independent triggers. The target detectors are housed in a nitrogen environment to prevent background events due to the diffusion of the radioactive radon gas.

2.1 Germanium Detector

As depicted in Figure 3a, the ULB-HPGe is surrounded by NaI(Tl) and CsI(Tl) crystal scintillators as anti-Compton detectors, and the whole set-up is further enclosed by another 3.5 cm of OFHC copper and lead blocks.

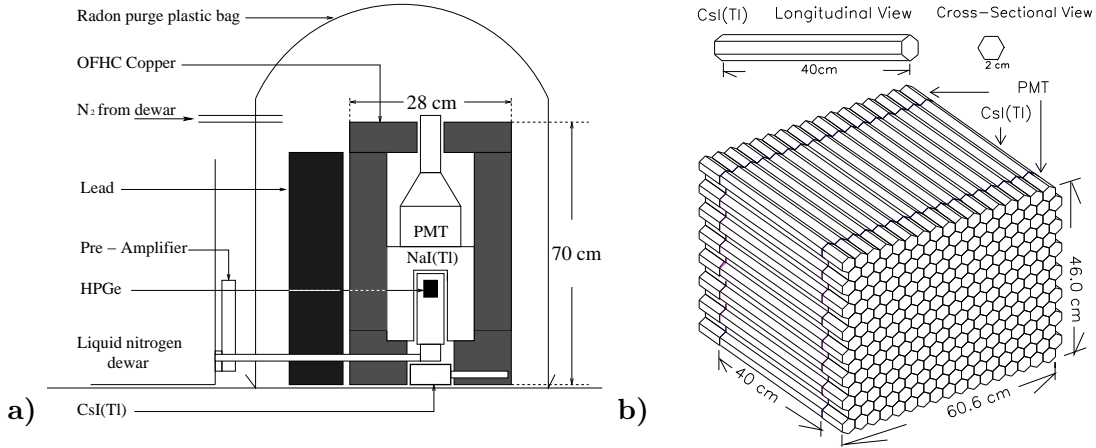


Figure 3: Schematic drawings of (a) the ULB-HPGe detector with its anti-Compton scintillators and passive shieldings; and (b) the CsI(Tl) target configuration where a total of 93 modules (186 kg) is installed for Period II.

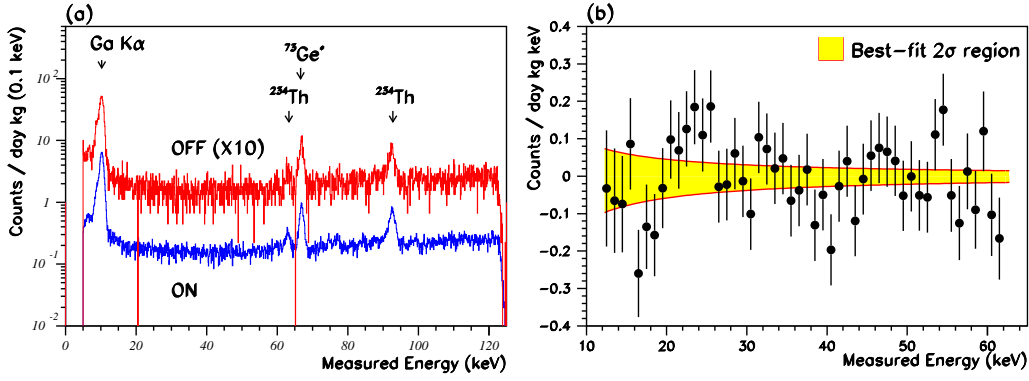


Figure 4: (a) The ON and OFF spectra after all identifiable background suppressed, for 4720 and 1250 hours of data, respectively. (b) The residual of the ON spectrum over the OFF background, with the 2- σ best-fit region overlaid.

After suppression of cosmic-induced background, anti-Compton vetos and convoluted events by pulse shape discrimination, the measured spectra for 4712/1250 hours of Reactor ON/OFF data in Period I[11] are displayed in Figure 4a. Background at the range of $1 \text{ keV}^{-1} \text{ kg}^{-1} \text{ day}^{-1}$ and a detector threshold of 5 keV are achieved. These are the levels comparable to underground Dark Matter experiment. Comparison of the ON and OFF spectra shows no excess and limits of the neutrino magnetic moment $\mu_{\bar{\nu}_e} < 1.3(1.0) \times 10^{-10} \mu_B$ at 90(68)% confidence level (CL) were set. The residual plot together with the best-fit regions are depicted in Figure 4b.

Depicted in Figure 5a is the summary of the results in $\mu_{\bar{\nu}_e}$ searches versus the achieved threshold in reactor experiments. The dotted lines denote the $R = \sigma(\mu)/\sigma(\text{SM})$ ratio at a particular $(T, \mu_{\bar{\nu}_e})$. The KS(Ge) experiment has a much lower threshold of 12 keV compared to the other measurements. The large R-values imply that the KS results are robust against the uncertainties in the SM cross-sections. The neutrino-photon couplings probed by μ_{ν} -searches in ν -e scatterings are related to the neutrino radiative decays (Γ_{ν})[12]. The indirect

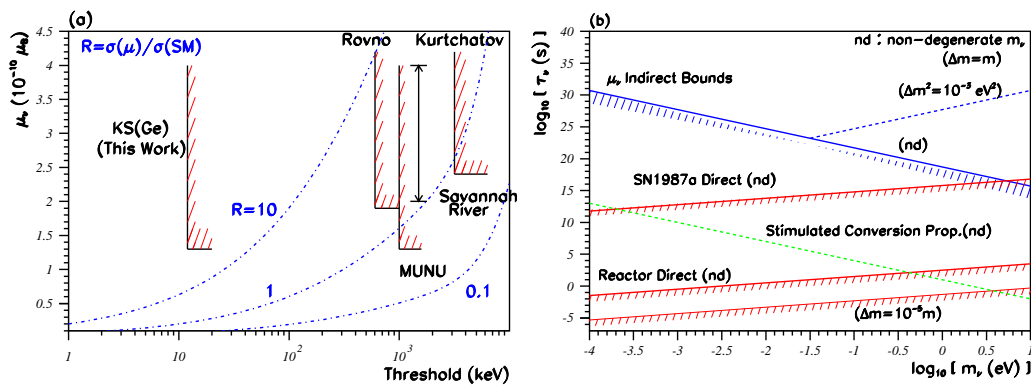


Figure 5: Summary of the results in (a) the searches of neutrino magnetic moments with reactor neutrinos, and (b) the bounds of neutrino radiative decay lifetime.

bounds on Γ_ν can be inferred and displayed in Figure 5b. It can be seen that ν -e scatterings give much more stringent bounds than the direct approaches.

The KS data with ULB-HPGe are the lowest threshold data so far for reactor neutrino experiments, and therefore allow the studies of several new and more speculative topics. Nuclear fission at reactor cores also produce electron neutrino (ν_e) through the production of unstable isotopes, such as ^{51}Cr and ^{55}Fe , via neutron capture, The subsequent decays of these isotopes by electron capture would produce mono-energetic ν_e . A realistic neutron transfer simulation has been carried out to estimate the flux. Physics analysis on the μ_ν and Γ_ν of ν_e will be performed, while the potentials for other physics applications will be studied. In additional, an *inclusive* analysis of the anomalous neutrino interactions with matter will be performed.

2.2 Scintillating CsI(Tl) Crystals

The potential merits of crystal scintillators for low-background low-energy experiments were recently discussed[5]. The CsI(Tl) detector configuration for the KS experiment is displayed in Figure 3b. Each crystal module is 2 kg in mass and consists of a hexagonal-shaped cross-section with 2 cm side and a length 40 cm. The light output are read out at both ends by custom-designed 29 mm diameter photo-multipliers (PMTs) with low-activity glass. The sum and difference of the PMT signals gives information on the energy and the longitudinal position of the events, respectively. A total of 186 kg (or 93 modules) have been commissioned for the Period II data taking. A major physics goal is the measurement of the Standard Model neutrino-electron scattering cross sections. The strategy[10] is to focus on data at high (>2 MeV) recoil energy. The large target mass compensates the drop in the cross-sections.

Extensive measurements on the crystal prototype modules have been performed[13]. The energy and spatial resolutions as functions of energy are depicted in Figure 6a and 6b, respectively. The energy is defined by the total light collection $\sqrt{Q_L * Q_R}$. It can be seen that a $\sim 10\%$ FWHM energy resolution is achieved at 660 keV. The detection threshold (where signals are measured at both PMTs) is <20 keV. The longitudinal position can

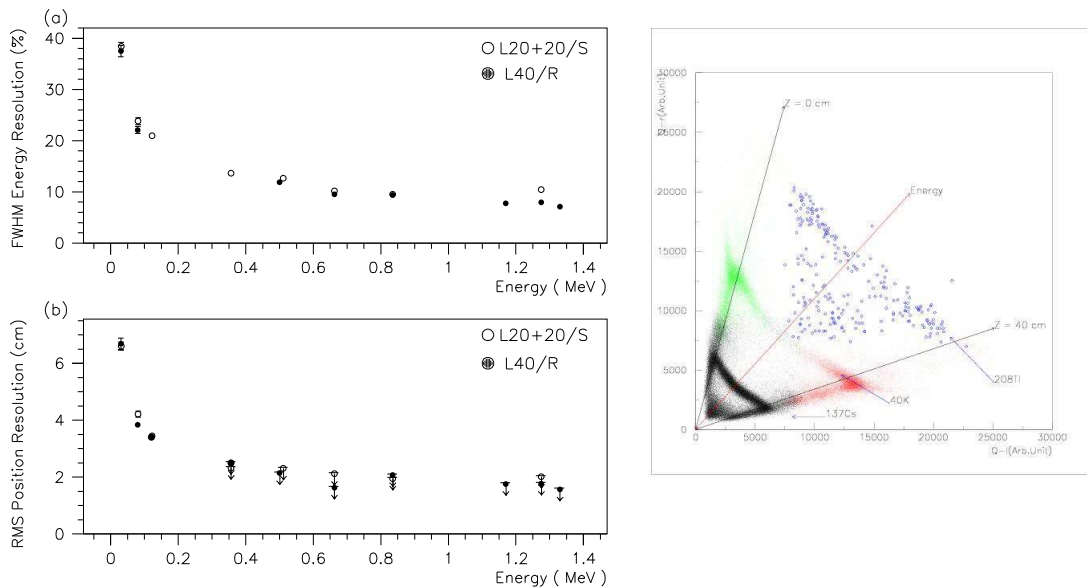


Figure 6: The variation of (a) FWHM energy resolution and (b) RMS position resolution with energy for the CsI(Tl) crystal modules. Only upper limits are shown for the higher energy points in (b) since the events are not localized. (c) Q_L versus Q_R distributions for single site events.

be obtained by considering the variation of the ratio $R = (Q_L - Q_R)/(Q_L + Q_R)$ along the crystal. Resolutions of ~ 2 cm and ~ 3.5 cm at 660 keV and 200 keV, respectively, have been demonstrated.

In addition, CsI(Tl) provides powerful pulse shape discrimination (PSD) capabilities to differentiate γ/e from α events, with an excellent separation of $>99\%$ above 500 keV. The light output for α 's in CsI(Tl) is quenched less than that in liquid scintillators. The absence of multiple α -peaks above 3 MeV [14] in the prototype measurements suggests that a ^{238}U and ^{232}Th concentration (assuming equilibrium) of $< 10^{-12}$ g/g can be achieved. It has been shown that PSD can also be achieved for pulse shapes which are partially saturated[8].

The typical Q_L versus Q_R distributions for single-site events after cosmic vetos are depicted in Figure 6c. There are evidence of contamination of internal radioactivity due to residual ^{137}Cs , such that the distributions of the 662-keV events are uniform across the 40 cm crystal length. Events due to γ -background from ^{40}K (1460 keV) and ^{208}Tl (2612 keV), on the other hand, occur more frequently near both edges, indicating that they are from sources external to the crystals. The background is very low above 2.6 MeV, making this a favorable range to provide a measurement of $\sigma(\text{SM})$.

A preliminary background energy spectrum of recoil electrons for central crystal and only one week OFF - period data sets are depicted in Figure 7. For this spectrum, initially we applied moderate cuts like single event hit, single crystal hit and cosmic ray cuts. After applying these cuts we were able to see ^{137}Cs and ^{40}K peaks. Further we applied a few specific cuts such as Alpha event cut and accidental event cut. Alpha events have very fast fall time compared to normal event and they are all located around 2.0 MeV. After

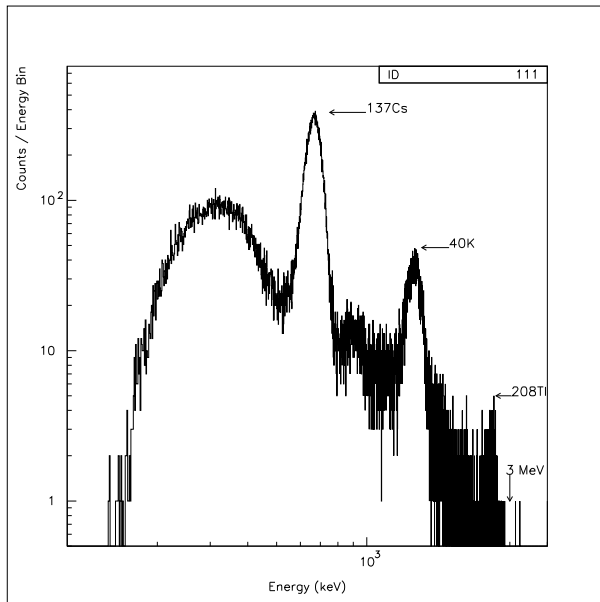


Figure 7: Background energy spectrum of recoil electrons.

applying these cuts the third peak of ^{208}Tl could be seen. In this spectrum we have not used z -position cuts. From this spectrum we can see that above 2.9 MeV there are only TWO data points and there is no data point above 3.5 MeV. Thus, the signal to background ratio is 1/17 above 3.0 MeV and this ratio must be better when we calculate in term of ON period data over OFF period data and applying z -position cut.

3. R&D Program

Various R&D projects with are proceeding in parallel to the KS reactor neutrino experiment. The highlights are:

3.1 Low Energy Neutrino Detection

It is recognized recently that ^{176}Yb and ^{160}Gd are good candidate targets in the detection of solar neutrino (ν_e) by providing a flavor-specific time-delayed tag[15]. Our work on the Gd-loaded scintillating crystal GSO[16] indicated major background issues to be addressed. We are exploring the possibilities of developing Yb-based scintillating crystals, like doping the known crystals $\text{YbAl}_5\text{O}_{12}$ (YbAG) and YbAlO_3 (YbAP) with scintillators.

The case of “Ultra Low-Energy” ULB-HPGe detectors, with the potential applications of Dark Matter searches and neutrino-nuclei coherent scatterings, is being investigated. As depicted in the measurement with a ^{55}Fe X-ray source on a 5 g prototype detector in Figure 8, a hardware energy threshold of better than 100 eV has been achieved. The lower energy peaks are those due to back-scattering of the X-rays from Ti. It is technically

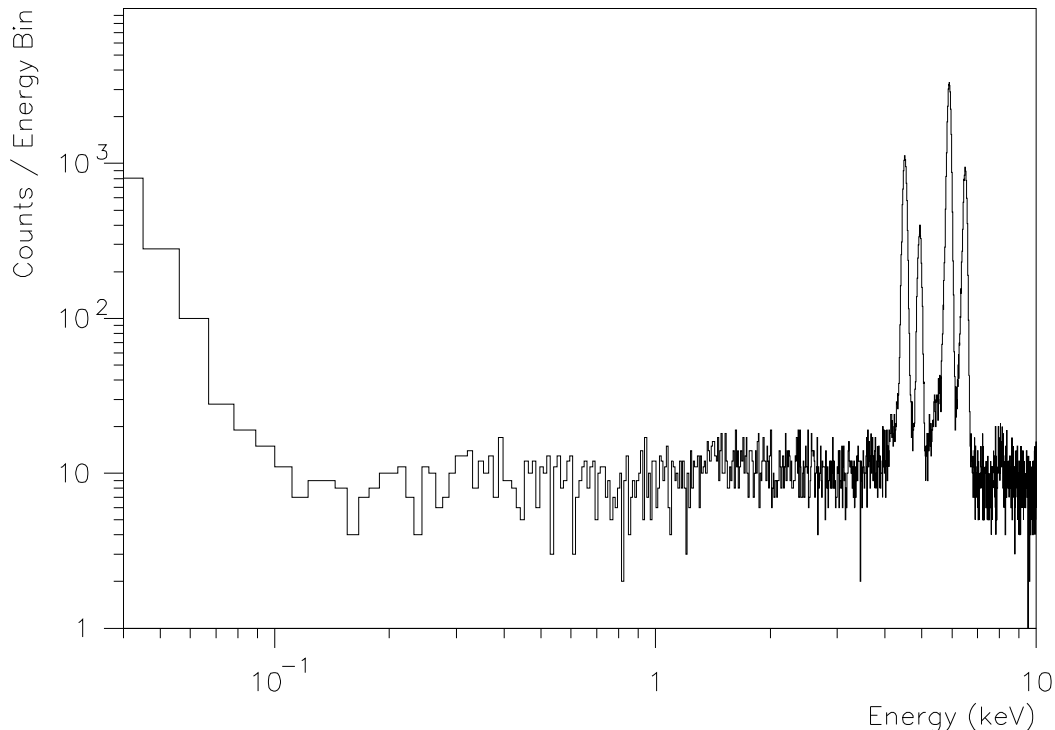


Figure 8: Measured spectrum with the ultra-low-energy HPGe detector exposed to a ^{55}Fe source. A threshold of better than 100 eV is achieved.

feasible to build an array of such detectors to increase the target size to the 1 kg mass range.

3.2 Dark Matter Searches with CsI(Tl)

Experiments based on the mass range of 100 kg of NaI(Tl) are producing some of the most sensitive results in Dark Matter “WIMP” searches[17]. The feasibilities and technical details of adapting CsI(Tl) or other good candidate crystal like $\text{CaF}_2(\text{Eu})$ for WIMP Searches have been studied. A neutron test beam measurement for CsI(Tl) was successfully performed at IAE 13 MV Tandem accelerator[18]. We have collected the lowest threshold data for nuclear recoils in CsI(Tl), enabling us to derive the quenching factors, displayed in Figure 9a, as well as to study the pulse shape discrimination techniques at the realistically low light output regime[19]. The measurements also provide the first confirmation of the Optical Model predictions on neutron elastic scatterings with a direct measurement on the nuclear recoils of heavy nuclei, as illustrated by the differential cross-section measurements of Figure 9b. A full scale Dark Matter experiment with CsI(Tl) crystals is being pursued by the KIMS Collaboration in South Korea[20].

3.3 Radio-purity Measurements with Accelerator Mass Spectrometry

Measuring the radio-purity of detector target materials as well as other laboratory com-

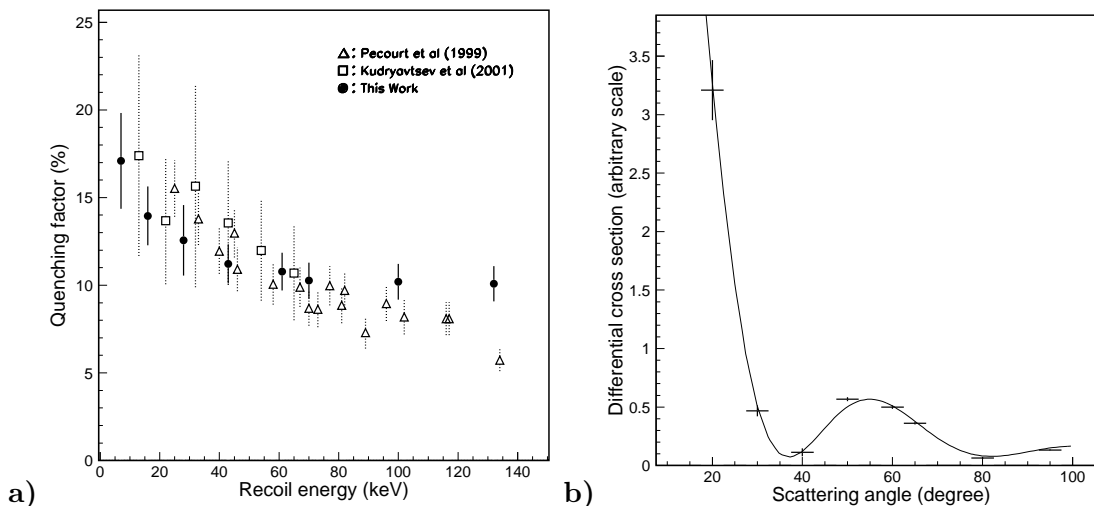


Figure 9: (a) The quenching factors, shown as black circles, measured at IAE Tandem, as compared to previous work. (b) The measured nuclear recoil differential cross sections in CsI(Tl), superimposed with the Optical Model predictions.

ponents are crucial to the success of low-background experiments. The typical methods are direct photon counting with high-purity germanium detectors, α -counting with silicon detectors, conventional mass spectrometry or the neutron activation techniques. We are exploring the capabilities of radio-purity measurements further with the new Accelerator Mass Spectroscopy (AMS) techniques[21]. This approach may be complementary to existing methods since it is in principle a superior and more versatile method as demonstrated in the ^{13}C system, and it is sensitive to radioactive isotopes that do not emit γ -rays (like single beta-decays from ^{87}Rb and ^{129}I) or where γ emissions are suppressed (for instance, measuring ^{39}K provides a gain of 10^5 in sensitivity relative to detecting γ 's from ^{40}K). A pilot measurement of the $^{129}\text{I}/^{127}\text{I}$ ratio ($< 10^{-12}$) in CsI was successfully performed demonstrating the capabilities of the Collaboration. Further beam time is scheduled at the IAE AMS facilities[22] to devise measuring schemes for the other other candidate isotopes like ^{238}U , ^{232}Th , ^{87}Rb , ^{40}K in liquid and crystal scintillators beyond the present capabilities by the other techniques. The first isotope to study is on ^{40}K , where the goal sensitivity of a 10^{-14}g/g should be achieve-able by the AMS techniques.

3.4 Upgrade of FADC for LEPS Experiment

Based on the design and operation of the FADCs at the KS experiment, we developed new FADCs for the Time Projection Chamber (TPC) constructed as a sub-detector for the LEPS experiment at the SPring8 Synchrotron Facilities in Japan[23]. The LEPS FADCs have 40 MHz sampling rate, 10-bit dynamic range, 32 channels per module and are equipped with Field Programmable Gate Array (FPGA) capabilities for real time data processing. The TPC has 1000 readout channels and a typical cosmic-ray event is depicted in Figure 10. The new system will be commissioned at LEPS in summer 2003. The upgraded FADCs will be further optimized and implemented to the KS reactor neutrino experiment for data taking in 2004.

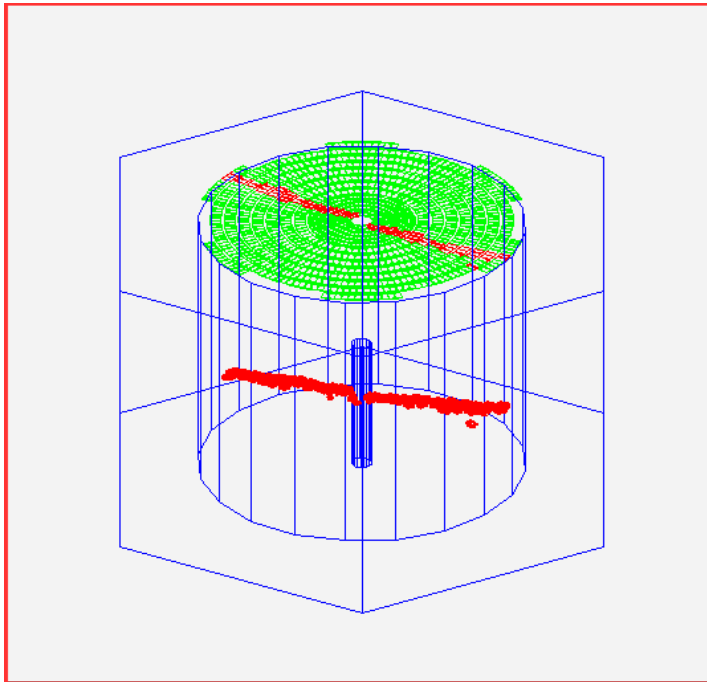


Figure 10: A typical cosmic-ray event recorded by the TPC for the LEPS Experiment, using an FADC-based data acquisition system.

4. Outlook

The strong evidence of neutrino masses and mixings[4] lead to intense world-wide efforts to pursue the next-generation of neutrino projects. Neutrino physics and astrophysics will remain a central subject in experimental particle physics in the coming decade and beyond. There are room for ground-breaking technical innovations – as well as potentials for surprises in the scientific results.

A collaboration among scientists from Taiwan and China has been built up with the goal of establishing a qualified experimental program in neutrino and astro-particle physics. It is the first generation collaborative efforts in large-scale basic research between scientists from Taiwan and China. The flagship effort is to perform the first-ever particle physics experiment in Taiwan at the Kuo-Sheng Reactor Plant. World-level sensitivities on the neutrino magnetic moment and radiative lifetime have already been achieved with the Period I data using a high-purity germanium detector. Further measurements are pursued at the Kuo-Sheng Laboratory, including the Standard Model neutrino-electron scattering cross-section as well as neutrino coherent scattering with the nuclei. A wide spectrum of R&D projects are being pursued in parallel.

The importance of the implications and outcomes of the experiment and experience will lie besides, if not beyond, neutrino physics.

5. Acknowledgments

The authors are grateful to the scientific members, technical staff and industrial partners of TEXONO Collaboration, as well as the concerned colleagues in our communities for the

many contributions which “make it happen” in such a short period of time. Funding are provided by the National Science Council, Taiwan and the National Science Foundation, China, as well as from the operational funds of the collaborating institutes.

References

- [1] Home Page at <http://hepmail.phys.sinica.edu.tw/~texono/>
- [2] C.Y. Chang, S.C. Lee and H.T. Wong, Nucl. Phys. **B** (Procs. Suppl.) **66**, 419 (1998).
- [3] D. Normile, Science **300**, 1074 (2003).
- [4] See the respective sections in *Review of Particle Physics*, Particle Data Group, Phys. Rev. **D** **66** (2002), for details and references.
For recent updates, see *Proc. of the XXth Int. Conf. on Neutrino Physics & Astrophysics*, eds. F. von Feilitzsch and N. Schmitz, Nucl. Phys. **B** (Proc. Suppl.) **118** (2003).
- [5] H.T. Wong et al., Astropart. Phys. **14**, 141 (2000).
- [6] H.T. Wong and J. Li, Mod. Phys. Lett. **A** **15**, 2011 (2000);
H.B. Li et al., TEXONO Coll., Nucl. Instrum. Methods **A** **459**, 93 (2001).
- [7] W.P. Lai et al., TEXONO Coll., Nucl. Instrum. Methods **A** **465**, 550 (2001).
- [8] Q. Yue et al., Nucl. Instrum. Methods **A** **511**, 408 (2003).
- [9] B. Kayser et al., Phys. Rev. **D** **20**, 87 (1979);
P.Vogel and J.Engel, Phys. Rev. **D** **39**, 3378 (1989).
- [10] H.B. Li and H.T. Wong, J. Phys. **G** **28**, 1453 (2002).
- [11] H.B. Li et al., TEXONO Coll., Phys. Rev. Lett. **90**, 131802 (2003).
- [12] G.G. Raffelt, Phys. Rev. **D** **39**, 2066 (1989).
- [13] Y. Liu et al., TEXONO Coll., Nucl. Instrum. Methods **A** **482**, 125 (2002).
- [14] U. Kilgus, R. Kotthaus, and E. Lange, Nucl. Instrum. Methods **A** **297**, 425, (1990);
R. Kotthaus, Nucl. Instrum. Methods **A** **329**, 433 (1993).
- [15] R.S. Raghavan, Phys. Rev. Lett. **78**, 3618 (1997).
- [16] S.C. Wang, H.T. Wong, and M. Fujiwara, Nucl. Instrum. Methods **A** **479**, 498 (2002).
- [17] R. Bernabei et al., Phys. Lett.**B** **480**, 23 (2000), and references therein.
- [18] M.Z. Wang et al., Phys. Lett. **B** **536**, 203 (2002).
- [19] S.C. Wu et al., physics/0307002, submitted to Nucl. Instrum. Methods **A** (2003).
- [20] H.J. Kim et al., Nucl. Instrum. Methods **A** **457**, 471 (2001).
- [21] D. Elmore and F.M. Phillips, Science **346**, 543 (1987).
- [22] S. Jiang et al., Nucl. Instrum. Methods **B** **52**, 285 (1990);
S. Jiang et al., Nucl. Instrum. Methods **B** **92**, 61 (1994).
- [23] T. Nakano, LEPS Coll., Nucl. Phys. **A** **684**, 71c (2001).